Analysis of slags using Laser Induced Breakdown Spectroscopy (LIBS)

Hervé K. Sanghapi[1], Krishna K. Ayyalasomayajula[1], Fang Y. Yueh[1], Jagdish P. Singh[1,2], Dustin L. McIntyre[3], Jinesh C. Jain[3], and Jinichiro Nakano[3]
[1]Institute for Clean Energy Technology, Mississippi State University, Starkville, MS 39759, USA
[2]Department of Physics, King Saud University, Riyadh, KSA
[3]National Energy Technology Laboratory (NETL), Pittsburgh, PA 15236, USA

Abstract

Feasibility of laser induced breakdown spectroscopy (LIBS) for the analysis of gasification slags was investigated by comparing LIBS results to the ICP-OES. A small amount of slag sample was placed on a double sided adhesive tape and analyzed for Al, Ca, Fe, Si, and V. Use of partial least squares regression (PLS-R) and univariate simple linear regression (SLR) calibration methods indicated that apart from V (accuracy upto $\pm$ 20%) the accuracy of analysis varies within 0.35-6.5% for SLR and 0.06-10% for PLS-R. A paired-sample t-test within the 95% confidence level yielded p-values greater than 0.05, meaning no appreciable statistical difference was observed between the univariate SLR with internal standardization and the multivariate PLS-R for most of the analytes. From the results obtained in this work, LIBS response varies depending on the element and the technique used for quantitative analysis. Simultaneous use of univariate calibration curves with internal standard (intensity ratio) and PLS regression in multi-elemental analysis can help reduce the matrix effect of slags associated to their high variation in concentration. Overall, these results demonstrate the capability of LIBS as an alternative technique for analyzing gasification slags. Estimated limits of detection for Al, Ca, Fe, Si and V were 0.167, 0.78, 0.171, 0.243 and 0.01 wt%, respectively.

1 Introduction.

Slag has been widely studied and proven useful in many industrial applications such as steel industry. It is used in metallurgical process to increase steel quality through mastering the chemical analysis of slag; as composition of steel melt is greatly influenced by chemical reactions of the melt with slag components[1]. Slag analysis is also of great importance in slagging gasification where carbon feedstocks are converted into electricity, chemical products and transport fuel[2][3].Environmental and economic challenges posed by the use of coal as feedstock, have called for alternatives such as petroleum coke (petcoke), biomass, and mixtures [4][5]. Development of reliable gasification technology depends on a good understanding of the influence of the feedstock mineral impurities on slag formation. Slag chemistry directly affects gasifier performance and its service life because of continuous interactions with protective lining materials during gasification and the viscous nature at exit. In some cases, slag could also be reused as feedstock [6]. Chemical analysis of these slags is often carried out using inductively coupled plasma - Optical emission spectroscopy (ICP-OES) [7]. This technique requires time consuming sample digestion and has imitations for the analysis of refractory samples resulting in incomplete digestion. This technique is also limited by lack of inline capabilities, significantly slowing feedback, thus impacts quality and productivity as it takes more time to make process and batch

adjustments. X-ray fluorescence spectroscopy (XRF) is termed as the state of art measuring technique for slag but the major difficulty with this technique is the well-known effects of absorption and/or enhancement related to the major element composition of samples and standards, as well as higher detection limits and the availability of suitable certified reference materials [8]. In order to reduce this time and favor online analysis, there is need to seek other analytical methods. Laser based methods seem to be of great importance for its simplicity and other features such as non-contact measurements with analyte, less destructive, high measuring speed, and little or no sample preparation. Laser induced breakdown spectroscopy (LIBS) is a spectrochemical analytical technique with the aforementioned features which permits multi-elemental analysis. LIBS has gained a lot of attention during the recent years as its scope of applications get wider from solid, liquid to gas analysis. There is a plethora of publications and books that elaborate on this versatile technique [9][10][11]. LIBS has previously been applied for multi-elemental analysis of slag samples from steel plant. Reported results were in agreement with XRF. Coefficient of determination $R^2$of 0.99 for the main analytes Ca, Si, and Fe of converter slag was achieved [12].

In the present work, considering the advantages offered by LIBS as mentioned above, we aim at presenting laser induced breakdown spectroscopy (LIBS) as an alternative method of analyzing gasification slags. Synthetic slags with chemistry falling within coal-petcoke mixed feedstock slags were prepared for the investigation. Elements under investigation are Al, Ca, Fe, Si and V.

2 Materials and Methods.

2.1 Experimental setup.

Fig.1 shows the experimental setup. A frequency doubled second harmonic Q-switched Nd:YAG laser (Quantel CFR400 20Hz, 7ns pulse width, 6mm diameter, 235mJ maximum) was used as an excitation source. With availability of a small amount of sample, a double sided tape glass slide was used on which sample was scattered and placed on a rotating platform to ensure laser beam hits on fresh spot. Laser beam was focused on sample surface through a 30cm focal length quartz lens and a right-angle prism. Spectra was collected with an Andor (Mechelle ME5000) broadband spectrometer (200–975 nm spectral range) through a 100 µm diameter optical fiber equipped with a pickup lens (Ocean Optics Inc. (OOI) Part No.74-UV). The latter was placed 5cm away from the sample and at 45^0 with respect to the beam axis. Andor Solis software was used for acquisition setup. The spectrograph was connected to a personal computer for data acquisition. All measurements reported herein were carried out with same gate delay, gate width, and laser pulse energy. These were respectively optimized to 3µs, 10µs and 67.5mJ. All spectra correspond to the accumulation of 50 laser shorts with each striking a fresh surface by rotating the sample. The resulting resolved spectra are used for qualitative and quantitative analysis. Plasma is characterized by evaluating plasma electron density and temperature from calcium lines. The Unscrambler X 10.3, OriginPro 2015, Veusz1.23.1, and excel 2013 were used for data analysis

2.2 Methods.

Quantitative analysis of LIBS is greatly affected by matrix effects and even more so when univariate calibration curves are used. Self-absorption and saturation are frequently observed and significantly influence the peak heights or areas of the analyte lines and thus affect the sensitivity of the curves from which unknown concentrations are to be derived [13][14][15]. Several methods

have been used to correct the matrix effects [16][17][18]. In this work we apply internal standardization and multivariate analyses (MVA) - partial least squares regression (PLS-R) to minimize the shot-to-shot fluctuations. The background corrected intensities used were selected according to Aydin *et al.* [19]. Atomic data of selected lines used for plasma characterization are referenced from NIST atomic data base [20]. Our results are compared to those obtained by inductively coupled plasma - Optical emission spectroscopy (ICP-OES) which we simply name as ICP.

2.3 Sample preparation.

The elemental composition of slag sample is listed in Table 1. Synthetic slags for this investigation were prepared by heating reagent grade powders of respective oxides (Al, Ca, Fe, Si and V) at 1425 °C for S1-7, 1575 °C for S8-12, and 1500 °C for the T1-4 series in a 64 mol.% CO – 36 mol.% CO_2 atmosphere for 3 days, followed by water quench. Upon water quenching, all the molten slags were vitrified. After drying the slag samples and grinding them into fine powders, a nominal mass of about 50mg of the sample was fused with ~1g of $Li_2B_4O_7$ and diluted to a final volume of 100mL using 5% HNO3 [21]. ICP analysis was performed using spectral lines Al 309.271, Ca 317.933, Fe 238.204, Si 251.611, and V 292.402. External calibration and internal standardization procedures [22] were utilized to quantify the analytes and based on the standard reference material (BIR-1) the accuracy of ICP analysis was within $\pm$ 7%. For LIBS analysis about 10 mg of powder sample was placed on a double sided adhesive tape glass slide.

3 Results and discussion.

3.1 Plasma characterization.

Plasma parameters such as temperature and electron density were evaluated. Boltzmann plot (Figure.2) for calcium lines Ca(II)396.84nm, Ca(I)430.25nm, and Ca(I)443.49nm(Table.2) yielded a temperature T_e= (5994±280)K. Different ionization levels were used in order to avoid lines with close excitation energy. This is to limit the effect of varying spectral response of the apparatus, as well as to minimize the sensitivity to small fluctuations in emission intensity [23]. Electron density of laser induced plasma ranges from 10^{16} to 10^{19} cm^{-3} and for this study, electron density was determined from Stark broadening which avoids the assumptions regarding LTE[23]. Spectral line Ca(422.67nm) was fitted using Lorentzian profile while the corresponding broadening coefficient at T=5000K was considered from Griem [24]. An average electron density N_e of $9.87x10^{17}cm^{-3}$±4.67% was observed for all samples.

3.2 Quantitative analysis.

Precision and accuracy of LIBS analysis are limited by matrix effects [11] [16]. Kraushaar *et al*.[25] observed that a variation in the major elemental composition of slag leads to matrix effects. These variations ultimately affect the ablation rate thus increasing the fluctuation in the emission lines and reducing the sensitivity of the instrument. Many studies have investigated matrix effects and its possible remedies using internal standardization and multivariate analysis [15][25][26][27]. In this paper, internal standardization is used for univariate calibration with Ca and Si as internal standards whereas PLS-R calibration models are used for MVA by considering spectral range for each element (Al, Ca, Fe, Si and V). Due to difference in concentration range of samples two sets of calibration curves were plotted. The first set included samples (S1-12) and the other set samples

(T1-4). In the case of (S samples), 10 samples were used for calibration and 2 for predictions. For (T samples), 4 were used for calibration and 1 for predictions.

3.2.1 Univariate simple linear regression (SLR).

Univariate calibration curves for the two sets of data are shown in (Figure.3) where intensity ratios are plotted against concentration ratios. Ca and Si were used as internal standards. Though the correlation coefficients R^2 are between 0.969 and 0.993, the best fit revealed the presence of outliers for certain elements notably vanadium. This can be seen from the reduced number of plotted point (Figure.3) where only 6 out of 10 samples were used for the calibration of V in (S samples). The presence of outliers can be attributed to the difficulties in minimizing shot to shot fluctuation in multi-elemental analysis by LIBS.

3.2.2 Multivariate partial least squares regression (PLS-R).

Figure.4 shows the PLS-R calibration models for Al, Ca, Fe, Si and V. It is observed that the R^2 values are almost equal to 1, revealing a strong correlation between the predictions and references. With slopes tending to 1 and validation (val) R^2 close to the calibration (cal) R^2, we can qualify this model as good enough for running our regression. Furthermore, calibration and validation best fits deviate very little from target line due to high value of R^2. Like in the univariate analysis, outliers were observed in the PLS-R calibration curve of vanadium.

3.3 Analytical figures of merit.

To evaluate the figures of merit of LIBS, predictive results from these two approaches are compared to those obtained by ICP. Measurement precisions and %accuracy error are evaluated. An approximation of the detection limits is calculated.

3.3.1 Comparative results of partial Least Square, univariate calibrations curves versus ICP

A comparison of LIBS and ICP results is shown in (Figure.5). Predictions were done with sample S1, S7, S12 and T4. LIBS results were obtained by using both SLR and PLS-R and reported as mean value of five measurements. In general the repeatability for the major elements in terms of relative standard deviation (RSD) (Table.3) for SLR and PLS-R are almost on a par except for Al and Ca. The percent accuracy error (Table.3) explains the deviation from the reference (ICP) values. Apart from V where the accuracy error is up to 20%, for both SLR and PLS-R, the accuracy error is within 0.35-6% for SLR and 0.06-10% for PLS-R. Since the accuracy varies depending on the technique used, a paired-sample t-test was performed within the 95% confidence level in order to find the significance of the mean difference between SLR and PLS-R. Overall, the difference of the population means was not significantly different from the test difference (0) as indicated by the p-values (Table.3) were greater than the significance level (0.05). This signifies that no appreciable statistical difference was observed using univariate SLR calibration with internal standardization and the multivariate PLS-R except for Ca (S12), Fe (S12), Fe (T4), and V (S7). Using the reference (ICP) values and the accuracy error to interpret the p-values for these elements, SLR performed better than PLS_R on Ca (S12) and Fe (S12) while PLS_R performed better than SLR on Fe (T4). As for V (S7) the paired-sample test could not be validated based on the high accuracy error with respect to the reference value. With the exception of V for which the accuracy error is about ±20%, the use of internal standardization and multivariate analysis have resulted in accuracy of up to 0.06% for other elements. Simultaneous use of univariate calibration curves with

internal standardization and PLS regression in multi-elemental matrix demonstrates the capability of LIBS as an alternative technique for analyzing gasification slags.

3.3.2 Limit of detection

The limit of detection (LOD) defined as *3CN/I* can be calculated from a spectrum with lowest analyzed concentration, where *N* is noise calculated from the standard deviation of the background near the analyzed line; *C* is the concentration of the analyzed line; *I* is the intensity of the analyzed line. Estimated limits of detection for Al, Ca, Fe, Si and V were 0.167, 0.78, 0.171, 0.243 and 0.01 wt% respectively.

4 Conclusion

In this work, spectrochemical analysis of gasification slags has been reported using laser induced breakdown spectroscopy (LIBS). Synthetic slags were prepared for investigating oxides of Al, Ca, Fe, Si, and V. Quantitative analyses were performed using univariate calibration curves and partial least square regression (PLS). Internal standardization was used in univariate (SLR) calibration curves to minimize the shot to shot variation in plasma. LIBS results were compared with those obtained by ICP and they were in accordance. From the results obtained in this work, LIBS response varies depending on the element and the technique used for quantitative analysis thus the simultaneous use of univariate calibration curves with internal standardization (intensity ratio) and PLS regression in multi-elemental analysis can help reduce the matrix effects of slags with high variation in elemental concentration. Though the calibration curves might give a correlation coefficient greater than 0.95, it is worth performing predictions and evaluating the accuracy errors. Overall, these results demonstrate the capability of LIBS as an alternative technique for analyzing gasification slags.

Acknowledgement

Mr. Hervé K. Sanghapi is thankful to Department of Physics, Mississippi State University for providing Graduate Teaching Assistantship.

5 References

[1] M. Kraushaar, R. Noll, and H. Schmitz, “Multi-elemental analysis of slag from steel production using laser induced breakdown spectroscopy,” *Int. Meet. Chem. Eng. …*, p. 2000, 2000.

[2] M. Aineto, A. Acosta, J. Rincon, and M. Romero, “Thermal expansion of slag and fly ash from coal gasification in IGCC power plant,” *Fuel*, pp. 2–11, 2006.

[3] M. Khosravi and A. Khadse, “Gasification of Petcoke and Coal/Biomass Blend: A Review,” *Int. J. Emerg. Technol. Adv. Eng.*, vol. 3, no. 12, pp. 167–173, 2013.

[4] S. Xu, Z. Zhou, X. Gao, G. Yu, and X. Gong, “The gasification reactivity of unburned carbon present in gasification slag from entrained-flow gasifier,” *Fuel Process. Technol.*, vol. 90, no. 9, pp. 1062–1070, Sep. 2009.

[5] T. Wu, M. Gong, E. Lester, F. Wang, Z. Zhou, and Z. Yu, “Characterisation of residual carbon from entrained-bed coal water slurry gasifiers,” *Fuel*, vol. 86, no. 7–8, pp. 972–982, May 2007.

[6] T. Powell, C., Bennett, J., Morreale, B., & Gardner, “Addressing the Materials Challenges in Converting Biomass to Energy,” vol. 110, 2011.

[7] I. M. Potgieter, “Analysis of Ferromanganese and Ferromanganese Slag by Means of Inductively Coupled Plasma Optical Emission Spectrometry *,” vol. 55, no. 12, 2001.

[8] A. Coedo and M. Dorado, “Approach to the solution of carbon content influence in the X-ray fluorescence analysis of ferromanganese,” *Appl. Spectrosc.*, vol. 698, p. 1994, 1994.

[9] A. Ciucci, M. Corsi, V. Palleschi, S. Rastelli, and A. Salvetti, “New Procedure for Quantitative Elemental Analysis by Laser-Induced Plasma Spectroscopy,” vol. 53, no. 8, pp. 960–964, 1999.

[10] J. P. Singh and S. N. Thakur, *Laser-induced breakdown spectroscopy*. Elsevier, 2007.

[11] D. Cremers and L. Radziemski, *Handbook of Laser–Induced Breakdown Spectroscopy*, 2nd ed. John Wiley & Sons, 2013.

[12] M. Kraushaar, R. Noll, and H. Schmitz, “Slag Analysis with Laser-Induced Breakdown Spectrometry,” *Appl. Spectrosc.*, vol. 57, no. 10, pp. 1282–1287, 2003.

[13] V. Lazic, R. Barbini, and F. Colao, “Self-absorption model in quantitative laser induced breakdown spectroscopy measurements on soils and sediments,” *Spectrochim. Acta - Part B At. Spectrosc.*, no. October 2000, 2001.

[14] S. Clegg, E. Sklute, and M. Dyar, “Multivariate analysis of remote laser-induced breakdown spectroscopy spectra using partial least squares, principal component analysis, and related techniques,” *Spectrochim. Acta - Part B At. Spectrosc.*, vol. 64, no. 1, pp. 79–88, Jan. 2009.

[15] C. Chaleard, P. Mauchien, and N. Andre, “Correction of matrix effects in quantitative elemental analysis with laser ablation optical emission spectrometry,” *J. Anal. …*, vol. 12, no. February, pp. 183–188, 1997.

[16] A. Miziolek, V. Palleschi, and I. Schechter, *Laser Induced Breakdown Spectroscopy: Fundamentals and Applications*. 2006.

[17] B. Sallé, J.-L. Lacour, P. Mauchien, P. Fichet, S. Maurice, and G. Manhès, “Comparative study of different methodologies for quantitative rock analysis by Laser-Induced Breakdown Spectroscopy in a simulated Martian atmosphere,” *Spectrochim. Acta Part B At. Spectrosc.*, vol. 61, no. 3, pp. 301–313, Mar. 2006.

[18] B. Praher, V. Palleschi, R. Viskup, J. Heitz, and J. D. Pedarnig, “Calibration free laser-induced breakdown spectroscopy of oxide materials,” *Spectrochim. Acta Part B At. Spectrosc.*, vol. 65, no. 8, pp. 671–679, Aug. 2010.

[19] Ü. Aydin, P. Roth, C. D. Gehlen, and R. Noll, “Spectral line selection for time-resolved investigations of laser-induced plasmas by an iterative Boltzmann plot method,” *Spectrochim. Acta Part B At. Spectrosc.*, vol. 63, no. 10, pp. 1060–1065, Oct. 2008.

[20] “http://physics.nist.gov/PhysRefData/ASD/lines_form.html.” .

[21] J.C. Jain, C. R. Neal, and J. M. Hanchar, “Problems associated with the determination of rare-earth elements in a ‘Gem’ quality zircon by ICP -MS,” *Geostand. Newsl.*, vol. 25, pp. 229–237, 2001.

[22] M. A. Schneegurt, J. C. Jain, J. A. Menicucci, S. A. Brown, K. M. Kemner, D. F. Garofalo, M. R. Quallick, C. R. Neal, and J. F. Kulpa, “Biomass byproducts for the remediation of wastewaters contaminated with toxic metals,” *Environ. Sci. Technol.*, vol. 35, no. 18, pp. 3786–3791, 2001.

[23] V. Palleschi, I. National, G. Cristoforetti, and I. National, “From sample to signal in laser-induced breakdown spectroscopy : A complex route to quantitative analysis From Sample to Signal in Laser Induced Breakdown Spectroscopy : A Complex Route to Quantitative Analysis,” in *Laser Induced Breakdown Spectroscopy: Fundamentals and Applications*, 2006, pp. 122–190.

[24] H. Griem, *Spectral line broadening by plasmas*. .

[25] M. Kraushaar, R. Noll, and H. U. Schmitz, “Slag analysis with laser-induced breakdown spectrometry.,” *Appl. Spectrosc.*, vol. 57, no. 10, pp. 1282–1287, Oct. 2003.

[26] J. Vrenegor, R. Noll, and V. Sturm, “Investigation of matrix effects in laser-induced breakdown spectroscopy plasmas of high-alloy steel for matrix and minor elements,” *Spectrochim. Acta Part B At. Spectrosc.*, vol. 60, no. 7–8, pp. 1083–1091, Aug. 2005.

[27] J. a. Aguilera, C. Aragón, V. Madurga, and J. Manrique, “Study of matrix effects in laser induced breakdown spectroscopy on metallic samples using plasma characterization by emission spectroscopy,” *Spectrochim. Acta Part B At. Spectrosc.*, vol. 64, no. 10, pp. 993–998, Oct. 2009.

Table 1 Concentration ranges of analytes in slag samples analyzed by ICP-OES

Sample (wt%)	Al	Ca	Fe	Si	V
S1	14.12	6.01	4.85	29.62	0.01
S2	10.55	6.26	2.64	35.11	0.93
S3	23.86	6.05	5.37	21.66	0.01
S4	9.66	6.01	2.54	31.97	2.90
S5	13.69	6.19	1.60	26.37	3.69
S6	15.10	5.61	2.57	22.49	6.38
S7	14.19	7.21	1.44	34.15	3.29
S8	12.49	5.84	2.21	31.71	0.01
S9	25.69	6.86	3.07	24.38	0.02
S10	25.95	7.42	4.51	24.24	6.07
S11	17.32	5.89	3.27	24.12	1.61
S12	19.03	6.60	3.05	25.55	4.19
T1	24.14	5.23	13.86	53.39	0.03
T2	20.93	5.09	12.45	47.07	10.97
T3	17.51	5.08	11.39	39.92	23.04
T4	9.68	5.25	8.32	27.28	46.65
T5	6.49	5.18	6.72	19.72	59.35

Table 2. Spectroscopic data of calcium

Lines	g_iA_{ij}	E_i - E_j	X_z	K_B	w
	($x10^8 s^{-1}$)	(eV)	(eV)	(eVK^{-1})	(nm)
Ca(II)396.84	0.7	0 - 3.12	6.11	$8.62x10^{-5}$	$4.84x10^{-4}$
Ca(I)422.67	6.54	0 - 2.93			
Ca(I)430.25	2.72	1.89- 4.78			
Ca(I)443.49	1.34	1.88- 4.68			

Table 3. Comparative LIBS and ICP results.

	LIBS (SLR)	LIBS (PLS)	ICP	RSD (%)		% Accuracy Error		Confidence & Significance level (95%, 0.05)		
wt%				SLR	PLS	SLR	PLS	t Statistic	DF	P value>|t|
Al_S1	13.20±1.91	14.27±0.71	14.12	14.49	5	6.49	1.1	1.95	4	0.123
Al_S12	18.96±1.98	18.99±0.17	19.03	10.42	0.9	0.35	0.19	0.03		0.976
Ca_S1	6.13±0.28	6.01±0.05	6.01	4.55	0.86	2.03	0.06	1.12		0.327
Ca_S12	6.48±0.33	5.92±0.07	6.6	5.14	1.2	1.85	10.24	3.51		0.025
Fe_S1	5.16±0.20	4.78±0.26	4.85	3.93	5.41	6.44	1.53	2.11		0.102
Fe_S12	2.93±0.05	3.26±0.13	3.05	1.84	3.94	3.65	7.07	8.04		0.001
Si_S1	30.18±1.77	29.14±1.86	29.62	5.88	6.39	1.86	1.63	1.21		0.293
Si_S12	26.54±2.00	27.51±2.43	25.55	7.53	8.84	3.9	7.67	0.67		0.54
V_S7	2.88±0.42	4.19±0.45	3.29	14.61	10.8	12.47	27.61	4.66		0.01
V_S12	3.27±0.39	3.26±0.13	4.19	11.88	3.94	21.95	22.2	0.05		0.962
Al_T4	11.21±2.10	10.11±0.20	9.68	18.71	1.97	15.83	4.4	1.26		0.277
Ca _T4	5.39±0.34	5.12±0.07	5.25	6.33	1.3	2.58	2.57	1.94		0.125
Fe_ T4	13.96±1.47	8.08±0.32	8.32	10.54	3.92	13.72	2.84	9.33		0.001
Si_ T4	27.22±3.74	21.18±3.74	27.28	13.74	11.63	0.24	17.96	2.22		0.09
V_ T4	37.85±10.49	36.67±8.84	46.65	27.72	24.12	18.87	21.38	0.2		0.854

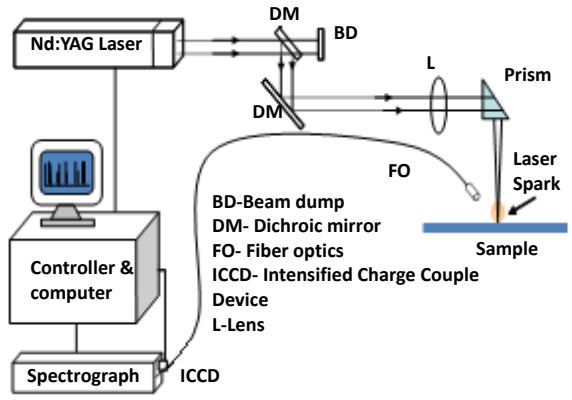

Figure 1. Experimental setup.

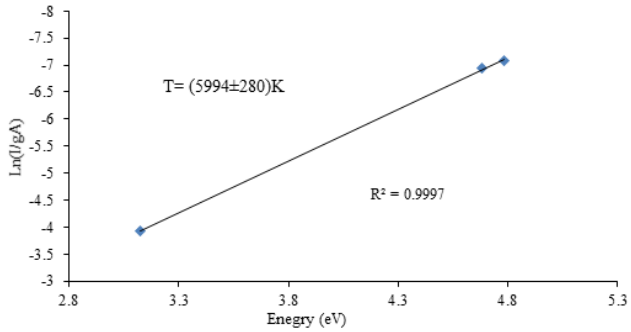

Figure 2. Boltzmann plot.

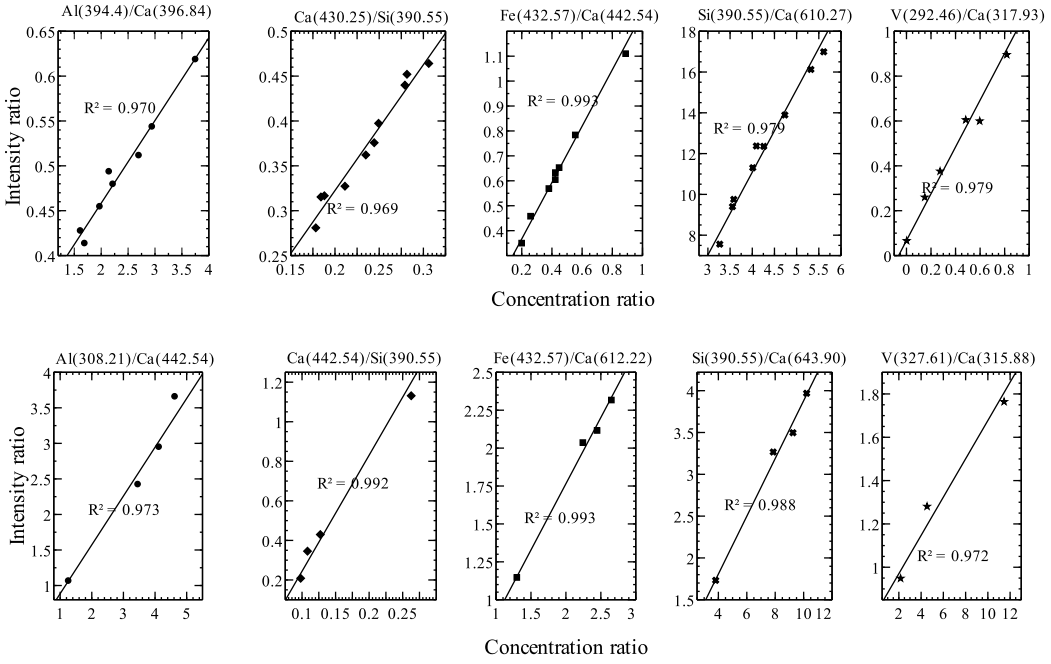

Figure 3. Simple linear calibration plots. Top (Sample set S) and bottom (Sample set T).

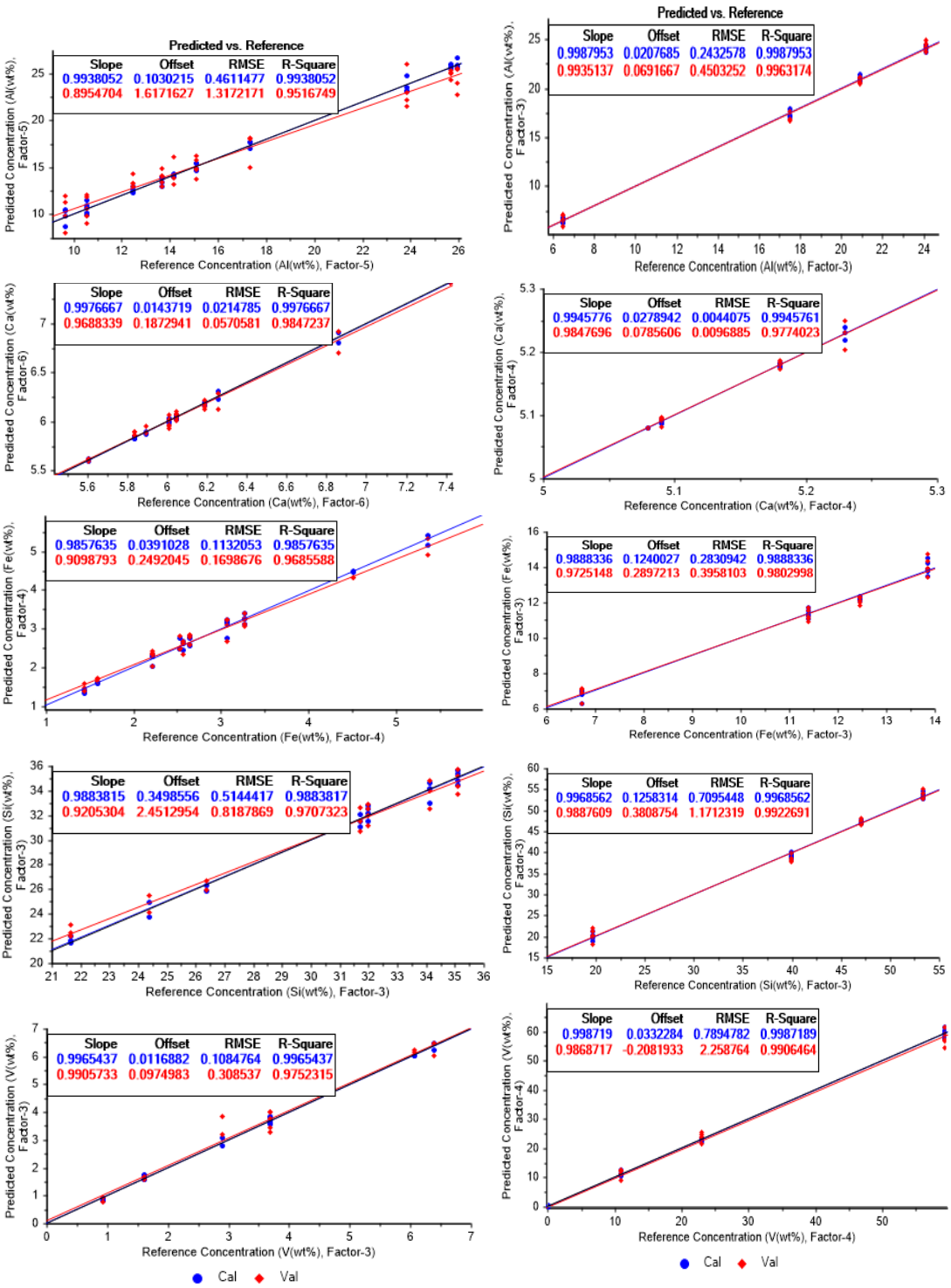

Figure 4. Partial least squares regression calibration. Left (Sample set S) and right (Sample set T).

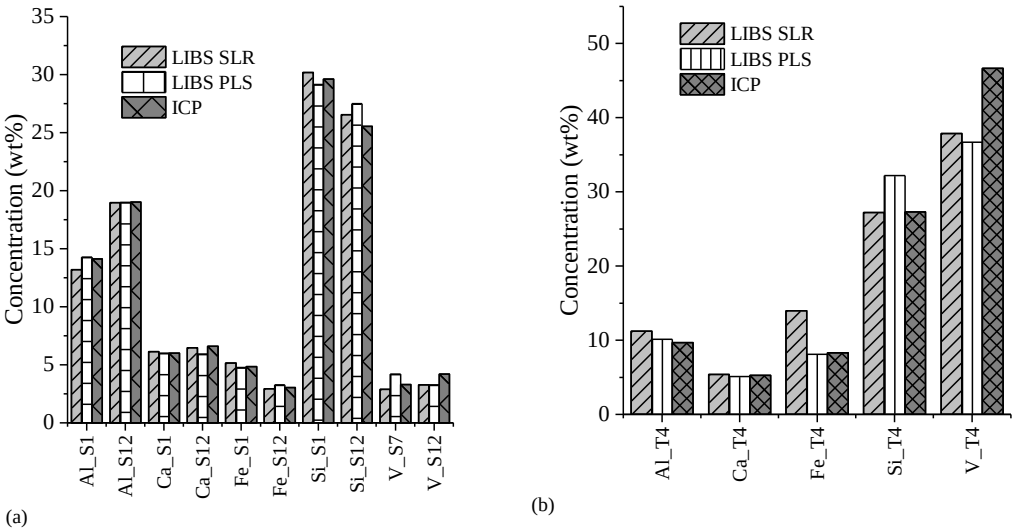

Figure 5. Comparison of LIBS (SLR&PLS-R) versus ICP-OES. Left (Sample set S) and right (Sample set T).